Structures, energetics, and spectra of fluoride–water clusters F − (H 2 O) n , n=1–6: Ab initio study

Jiwon Baik, Jongseob Kim, D. Majumdar, and Kwang S. Kim

Citation: The Journal of Chemical Physics **110**, 9116 (1999); doi: 10.1063/1.478833
View online: http://dx.doi.org/10.1063/1.478833
View Table of Contents: http://scitation.aip.org/content/aip/journal/jcp/110/18?ver=pdfcov
Published by the AIP Publishing

Structures, energetics, and spectra of fluoride–water clusters $F^-(H_2O)_n$, $n=1-6$: *Ab initio* study

Jiwon Baik, Jongseob Kim, D. Majumdar, and Kwang S. Kim[a)]
National Creative Research Initiative Center for Superfunctional Materials, Department of Chemistry Pohang, University of Science and Technology, San 31, Hyojadong, Namgu, Pohang 790-784, Korea

(Received 9 November 1998; accepted 10 February 1999)

$F^-(H_2O)_n$ ($n=1-6$) clusters have been studied using *ab initio* calculations. This is an extensive work to search for various low-lying energy conformers, for example, including 13 conformers for $n=6$. Our predicted enthalpies and free energies are in good agreement with experimental values. For $n=4$ and 6, both internal and surface structures are almost isoenergetic at 0 K, while internal structures are favored with increasing temperature due to the entropic effect. For $n=5$, the internal structure is favored at both 0 and 298 K under 1 atm. These are contrasted to the favored surface structures in other small aqua–halide complexes. The ionization potential, charge-transfer-to-solvent (CTTS) energy, and O–H stretching vibrational spectra are reported to facilitate future experimental work. Many-body interaction potential analyses are presented to help improve the potential functions used in molecular simulations. The higher order many-body interaction energies are found to be important to compare the energetics of the various conformers and compare the stability of the internal over the surface state. © *1999 American Institute of Physics.* [S0021-9606(99)30318-4]

I. INTRODUCTION

The emergence of diverse physical properties of aqua ions as a function of cluster size has attracted the intense attention of both experimentalists[1–10] and theorists in molecular and cluster physics.[11–26] The study of small aqueous ion clusters provides a way to probe the fundamental interactions that are responsible for solvation phenomena at the molecular level. The molecular orbital (MO) calculations at the *ab initio* level are a powerful tool for providing information regarding the structure and energetics of these systems. The results obtained through such calculations are important in supplementing experimental data and are even helpful to determine the accuracy of several sets of conflicting experimental results.

Ab initio predicted energetics of aqua–cation clusters, in contrast to aqua–anion clusters, have shown good agreement with experimental results.[24–26] The disagreement of the theoretical and experimental quantities for the latter case is partly due to conflicting experimental data.[7,8] The structures of aqua–halide anion clusters have long been the subject of controversy regarding internal or surface state of a halide anion.[2,13–23] This is similar to the problem of excess electron in water clusters.[27–29] From an analysis of the photoelectron spectroscopy of the clusters of halide ions in water, $X(H_2O)_n$ [$X=Cl^-, Br^-, I^-$], Cheshnovsky and his co-workers[2] have shown that surface structures are favored for $X=Cl^-$ and Br^- for small n, while for $X=I^-$, the $n=6$ cluster has an internal state with the first solvation layer coordination number of 6. However, they also suggested a surface solvation phenomenon to be operative in I^- solvation by fitting the experimental binding energies of large $I^-(H_2O)_n$ cluster to their models of classical electrostatic solvation.[2] The *ab initio* studies on $X^-(H_2O)_n$ clusters [X=Cl, Br, I, and $n=1-6$] by Combariza *et al.*,[13] have indicated that for $n=2-6$, the anion resides on the surface for Cl^- and Br^- clusters. For $I^-(H_2O)_n$ clusters this feature was also observed for $n=2-5$, while $I^-(H_2O)_6$ clusters showed the possibility of transition from surface to interior structure. On the other hand, various molecular dynamics (MD),[19–21] Monte Carlo,[22] and perturbative Monte Carlo[23] studies have shown the preference of the surface structures over the internal structures not only for the small anion–water clusters, but also in the case of medium-sized clusters such as $n=15$.

The structure of $F^-(H_2O)_n$ could be different from other aqua–halide anions X^- (X=Cl, Br, I), since the coulombic interaction between F^- and water is much stronger than that between X^- and water. Thus, in the case of F^-, probably the smallest number of water molecules would be needed to form an internal structure among the aqua–halide clusters. Earlier *ab initio* studies on $F^-(H_2O)$ included the work of Clementi and co-workers[11] and a very accurate calculation by Schaefer and co-workers.[12] The cluster structures of $F^-(H_2O)_n$ for $n=1-6$ were studied by Combariza and Kestner[14] with Möller-Plesset second-order perturbation (MP2) calculations at the Hartree–Fock (HF) optimized geometries using the 6-31+G* basis set. They have carried out quite exhaustive calculations on $F^-(H_2O)_n$ clusters and have concluded that a transition from predominant surface state to an interior state could be observed at $n=4$ and 5. The structural analysis of the $F^-(H_2O)_n$ ($n=1-3$) clusters was also done by Xantheas *et al.*[15] at the MP2/aug-cc-pVDZ level. They further reported the $F^-(H_2O)_n$ clusters which are in favor of the internal structures for $n=1-10$, using MD

a)Author to whom correspondence should be addressed. Electronic mail: kim@postech.ac.kr

simulation based on the *ab initio* fitted potentials and polarizable water potential.[17] Recently, Bryce *et al.* have reported quantum-mechanical/molecular-mechanical (QM/MM) studies of $F^-(H_2O)_4$ clusters.[18] Despite all these theoretical calculations, no extensive reliable *ab initio* studies are yet available for $n=5$ and 6 for which there could be a number of low-lying energy structures. We have, therefore, carried out a theoretical study of $F^-(H_2O)_n$ $[n=1-6]$ with a view to understand the nature of interaction that stabilizes the formation of internal or surface structure of these clusters at different ''*n*'' by locating the structures which reproduce the available experimental enthalpies and free energies.[7,8] In the present analysis of $F^-(H_2O)_n$ clusters, we have carried out density functional and MP2 calculations to analyze the $n=5$ and 6 cluster structures with much more geometrical possibilities than those used in the previous studies, and have predicted the lowest energy structures and thermal quantities. We have shown that our thermodynamic quantities are in good agreement with the experimental values, and internal structures are favored at room temperature for $n=4$ and 6 clusters due to the entropic effect. For $n=5$, the internal structure is favored at 0 K, when zero-point energy (ZPE) correction is made. The ionization potential, CTTS energies,[10] many-body interaction terms, and OH stretching spectra of the clusters are also discussed. It is to be mentioned in this connection that the conformational space for $n=4-6$ clusters as presented here for calculating their thermodynamic properties could not be considered to be complete because of the large structural possibilities of such clusters. On the other hand, consideration of the larger number of structural possibilities of these clusters with respect to the previous quantum chemical calculations and our success in calculating the experimentally measured thermodynamic quantities to near accuracy using such structural space, indicate the importance of our approach, especially, towards the weak clusters like $F^-(H_2O)_n$.

II. METHODS OF COMPUTATION

The geometries of all the $F^-(H_2O)_n$ clusters $(n=1-6)$ were fully optimized using HF, density functional, and MP2 theory without imposing any geometrical constraint. The density functional approaches have used Becke's exchange functional and the nonlocal functional by Lee, Yang, and Parr (in short, BLYP).[30] In HF calculations, the water molecules were represented by standard 6-31+G* basis sets and a double-ζ basis set of Mclean–Chandler[31] for the fluoride anion. This choice of basis set was made in accordance with the work of Combariza and Kestner,[14] so that the HF results presented here could be comparable. These HF calculations were used in order to locate the number of possible low-lying energy conformers. A 6-311++G** basis set was adopted for both water and fluoride ion at BLYP and MP2 levels. The basis set superposition error (BSSE) corrections (ΔBSSE) to the interaction energy for the optimized structures were estimated using the counterpoise method of Boys and Bernardi.[32] From the BLYP/6-311++G** frequency analysis of the different geometries of the fluoride–water clusters, zero-point energy (ZPE) corrections (ΔZPE) are made on the total energies, and the cluster energies are expressed at different level of corrections, *viz.*, as interaction energy (ΔE_e), $\Delta E_e+\Delta\mathrm{BSSE}(\Delta E_e^B)$, $\Delta E_e+\Delta\mathrm{ZPE}(\Delta E_0)$, and $\Delta E_e+\Delta\mathrm{BSSE}+\Delta\mathrm{ZPE}(\Delta E_0^B)$. The interaction energies are further used to modify the thermodynamic quantities, *viz.*, change of enthalpy (ΔH) and change of Gibbs free energy (ΔG) for the clusters. Throughout our calculations, the ZPE and thermal energies are used at the BLYP level. In most cases, the values of ΔZPE tend to be less dependent on the calculation methods employed due to the cancellation effect in ZPE errors between two systems investigated, even when the absolute ZPEs are somewhat different.[33]

In cases when basis sets employed are reasonably balanced, the binding energies (BEs, the negative values of the interaction energies) without ΔBSSE tend to be overestimated, while those with BSSE correction tend to be underestimated. The median values between the BSSE-corrected and BSSE-uncorrected BEs are often somewhat closer to the experimental values.[24,34] However, for the $F^-(H_2O)_n$ system, we find that the BSSE-uncorrected BEs are close to the experimental quantities, while the BSSE-corrected BEs seriously underestimate these values. This situation was often observed in a number of systems.[26,33,35] Although the BSSE can be important to evaluate the absolute BEs, its effect is generally not too significant on relative energy differences between different conformers.[33,36] This is also noted in our present study. Furthermore, since the MP2/6-311++G** results are regarded to be more reliable than the BLYP/6-311++G** results, and the BSSE-uncorrected results for the present system are in much better agreement with the experimental thermodynamic quantities, our discussion in this connection will be based on the BSSE-uncorrected MP2/6-311++G** results unless otherwise specified.

Entropy depends mainly on the intermonomeric vibrational modes, which were transformed from the rotational and translational motions of monomers upon complexation. Although ΔG is sensitive to the anharmonicity of low frequencies, the contributions from the 1st- and 2nd-order anharmonicities in Morse-type potentials or the like tend to cancel it partly. This could be noted from our previous accurate derivation.[33] Thus, the entropy evaluated even with harmonic approximation tends to be in good agreement with experimental values, and sometimes in much better agreement than expected.[24,33] However, when the frequencies are very low, the deviations could be quite significant. Indeed, serious error in free energy arises from the overestimated entropy corresponding to very low frequencies (in particular, $<10\ \mathrm{cm}^{-1}$ at room temperature and 1 atm). In this case, the vibrational motion in a very shallow harmonic potential needs to be replaced by the internal translational or hindered rotational motion of mono-, di-, or multi-water molecules, or submolecular systems of the complex, as the former entropy is much higher than the maximum of the latter entropies. Thus, in our calculation each vibrational entropy greater than the maximum value of the translational and rotational entropies of the water monomer has been replaced, as an approximation, by the latter. In this way, the unrealistic overestimation due to the harmonic assumption for low vibrational frequencies was avoided, and thus the entropies and free en-

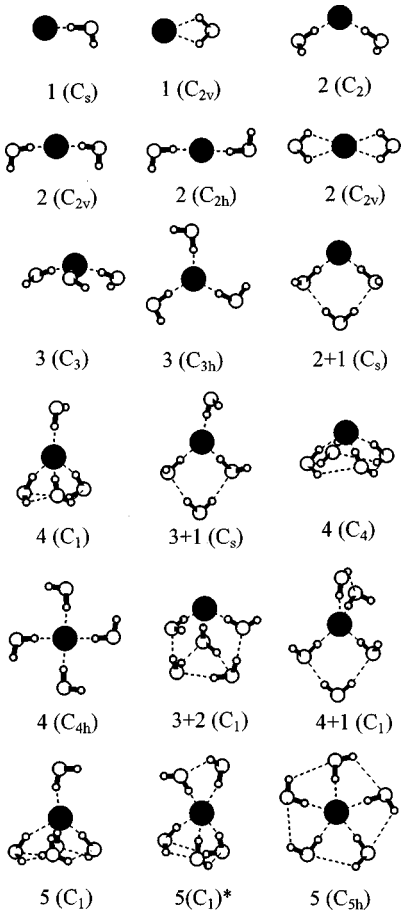

FIG. 1. Optimized geometries (MP2) for the $F^-(H_2O)_n$, $n=1-5$, clusters.

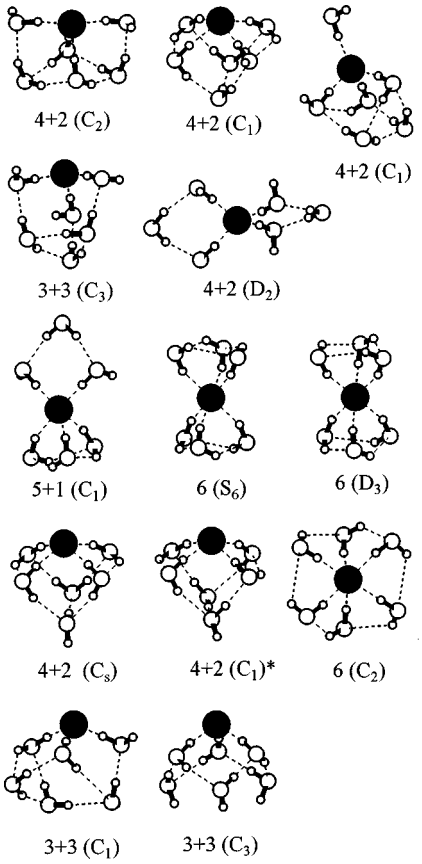

FIG. 2. Optimized geometries (MP2) of the $F^-(H_2O)_6$ cluster.

ergies calculated therefrom were more realistic. In our calculation, ΔG and ΔS of the chiral molecules were further corrected by $-RT\ln 2$ and $R\ln 2$, respectively[37] ($T=298$ K and R, the gas constant).

In case of small polar water clusters, hydrogen bonding between the water molecule plays a dominant role to determine their structures.[36,38] The interaction is more complex in the case of anionic clusters. In $F^-(H_2O)_n$ clusters, generally the dipole orientation is disfavored due to small F–O distances, while the H–O orientation in the clusters would be strengthened due to strong coulomb interaction with the F^- ion. This type of interaction will lead to asymmetric structures for $F^-(H_2O)$ clusters. In the present calculations for $n=1$ to 5, all the geometries considered by Combariza and Kester[14] were used as the starting geometry; a few other structures were also considered (Fig. 1). In the case of $n=6$, the structural possibilities could be very large. Altogether, 13 such structural possibilities have been considered (Fig. 2). They were mostly chosen from the low-energy structures of our anionic water clusters[29] and the low-energy $F^-(H_2O)_6$ clusters of Combariza and Kestner.[14] Frequency calculations were carried out on the optimized cluster geometries to ascertain the local minima, to differentiate them from the transition states, and to obtain the ZPEs and thermal quantities. All the calculations were carried out using a GAUSSIAN-94/GAUSSIAN-98 suite of programs.[39,40] To get further insight for the stability of the various low-energy clusters over the higher energy ones, the many-body interaction energies were analyzed.

III. RESULTS AND DISCUSSION

A. Energetics and structures

The optimized geometries of the various structural arrangements of $F^-(H_2O)_n$ $[n=1-6]$ are presented in Figs. 1 and 2. Figure 1 contains the structural arrangements of the $F^-(H_2O)_n$ clusters for $n=1-5$, while Fig. 2 represents various optimized structural arrangements of the $F^-(H_2O)_6$ cluster. The notation of each structure is represented by the coordination number (n_1+n_2), with the symmetries presented within parentheses. Here, n_1 and n_2, respectively, denote the number of water molecules in the primary and secondary hydration shells, and consequently when $n_2=0$, the structure is simply represented as n_1. The HF/6-31G*, BLYP/6-311++G**, and MP2/6-311++G** interaction energies (ΔE_e^B, ΔE_e, ΔE_0) for the $F^-(H_2O)_n$ clusters are presented in Table I, along with ΔH and ΔG. The geometrical parameters for the optimized cluster arrangements are presented in Table II.

In the case of $F^-(H_2O)$ cluster, the minimum energy structure is $1(C_s)$. The other structure, $1(C_{2v})$ with the F^- ion lying on the bisector of the H–O–H bond angle, was found to be a transition state, which connects two equivalent C_s structures of $F^-(H_2O)$ cluster. The geometries of the minimum energy cluster $1(C_s)$, as presented in Table II, indicate that the water structure is considerably distorted.

TABLE I. Binding energies ($-\Delta E_e$), ZPE-corrected energies ($-\Delta E_0$) at 0 K, enthalpies ($-\Delta H$), and Gibbs' free energies ($-\Delta G$) at 298 K and 1 atm for the various low energy $F^-(H_2O)_n$ clusters ($n=1-6$).[a]

			BLYP/6-311++G**				MP2/6-311++G**			
n	Structure	HF^b $-\Delta E_e$	$-\Delta E_e(-\Delta E_e^B)$	$-\Delta E_0(-\Delta E_0^B)$	$-\Delta H(-\Delta H^B)$	$-\Delta G(-\Delta G^B)$	$-\Delta E_e(-\Delta E_e^B)$	$-\Delta E_0(-\Delta E_0^B)$	$-\Delta H(-\Delta H^B)$	$-\Delta G(-\Delta G^B)$
1	$1(C_s)$ H-bonded	24.5	28.8 (26.7)	28.2 (26.1)	29.3 (27.2)	22.7 (20.7)	27.4 (24.4)	26.8 (23.8)	28.0 (25.0)	21.4 (18.4)
	$1(C_{2v})$ bifurcated		22.1 (19.2)	21.2 (18.3)	22.3 (19.4)	15.4 (12.6)	20.8 (18.9)	19.8 (17.9)	21.0 (19.1)	14.1 (12.2)
2	$2(C_2)$ bent[c]	44.6	50.3 (46.9)	47.6 (44.2)	49.0 (45.6)	36.3 (32.9)	49.2 (43.9)	46.4 (41.1)	47.9 (42.6)	35.2 (29.9)
	$2(C_{2v})$ linear	44.2	50.0 (46.7)	47.2 (44.0)	49.1 (45.8)	34.3 (31.1)	48.8 (43.7)	46.0 (40.9)	47.9 (42.8)	33.2 (28.1)
	$2(C_{2h})$ linear		50.2 (46.8)	47.3 (44.0)	48.7 (45.3)	35.7 (32.4)	48.6 (44.0)	45.8 (41.2)	47.1 (42.5)	34.2 (29.6)
	$2(C_{2v})'$ bifurcated		40.1 (36.2)	38.0 (34.1)	39.9 (36.1)	25.8 (21.9)	38.8 (35.1)	36.6 (32.9)	38.6 (34.9)	24.4 (20.8)
3	$3(C_3)$ surface[c]	62.0	67.7 (63.0)	62.8 (58.1)	64.5 (59.9)	44.1 (39.5)	67.4 (60.1)	62.5 (55.2)	64.3 (56.9)	43.9 (36.5)
	$3(C_{3h})$ planar		67.6 (63.2)	62.9 (58.5)	65.1 (60.7)	43.2 (38.8)	67.4 (60.1)	62.7 (55.4)	64.9 (57.6)	43.0 (35.7)
	$2+1(C_s)$ surface		67.1 (62.3)	61.1 (56.3)	63.8 (59.0)	39.3 (34.5)	66.9 (58.5)	60.9 (52.5)	63.6 (55.2)	39.1 (30.7)
4	$4(C_1)$ internal[c]	76.9	82.2 (75.8)	73.9 (67.5)	76.6 (70.3)	46.2 (39.9)	83.8 (74.0)	75.5 (65.7)	78.3 (68.4)	47.9 (38.1)
	$3+1(C_s)$ trisolvated		82.7 (76.4)	74.6 (68.4)	77.5 (71.3)	46.4 (40.2)	83.6 (73.1)	75.6 (65.0)	78.4 (67.9)	47.3 (36.8)
	$4(C_4)$ surface[c]	76.0	81.0 (74.7)	72.0 (65.7)	75.1 (68.8)	42.2 (35.9)	83.3 (73.4)	74.3 (64.5)	77.4 (67.6)	44.5 (34.6)
	$4(C_{4h})$ planar		80.1 (75.2)	73.4 (68.4)	76.4 (71.4)	44.1 (39.1)	80.8 (73.1)	74.0 (66.4)	77.0 (69.4)	47.8 (37.1)
5	$3+2(C_1)$ surface[c]	90.3	97.5 (89.8)	85.3 (77.6)	89.9 (82.1)	45.9 (38.1)	99.4 (85.7)	87.2 (73.4)	91.7 (78.0)	47.8 (34.0)
	$4+1(C_1)$ internal[c]		96.4 (89.1)	85.7 (78.4)	89.1 (81.8)	49.4 (42.2)	98.9 (86.5)	88.2 (75.8)	91.6 (79.2)	51.9 (39.5)
	$5(C_1)$ internal[c]	89.2	94.1 (86.7)	83.1 (75.7)	86.5 (79.1)	47.2 (39.7)	97.8 (85.7)	86.7 (74.7)	90.1 (78.0)	50.8 (38.7)
	$5(C_1)^*$ internal[c]	89.4	93.9 (86.5)	82.9 (75.5)	86.3 (78.9)	46.4 (39.0)	97.0 (85.4)	86.0 (74.4)	89.4 (77.7)	49.5 (37.9)
	$5(C_{5h})$ planar		89.1 (83.1)	80.0 (74.0)	84.0 (77.9)	40.8 (34.8)	93.1 (83.2)	84.0 (74.2)	88.0 (78.1)	44.8 (34.9)
6	$4+2(C_2)$ surface[c]	105.5	112.0 (102.9)	96.6 (87.4)	101.3 (92.1)	46.7 (37.5)	115.9 (99.7)	100.4 (84.2)	105.7 (89.6)	51.1 (35.0)
	$4+2(C_1)'$ surface[c]	103.7	110.4 (101.1)	94.9 (85.6)	99.7 (90.4)	45.4 (36.1)	114.7 (98.2)	99.2 (82.7)	104.6 (88.1)	50.3 (33.8)
	$4+2(C_1)$ internal[c]	103.7	110.6 (101.9)	96.5 (87.8)	100.5 (91.8)	49.8 (41.2)	114.1 (98.4)	100.0 (84.3)	104.6 (88.9)	53.9 (38.2)
	$3+3(C_3)$ surface[c]	102.5	110.7 (101.7)	96.2 (87.2)	100.7 (91.7)	47.2 (38.3)	113.5 (96.7)	99.0 (82.2)	104.1 (87.3)	50.6 (33.8)
	$4+2(D_2)$ internal[c]	102.7	109.0 (100.8)	95.5 (87.3)	99.1 (90.9)	49.1 (40.9)	112.3 (97.5)	98.8 (84.0)	102.9 (88.2)	53.0 (38.2)
	$5+1(C_1)$ internal[c]	101.9	106.8 (98.2)	93.3 (84.8)	96.9 (88.3)	46.9 (38.3)	111.3 (96.9)	97.8 (83.4)	102.0 (87.6)	52.0 (37.6)
	$6(S_6)$ internal	101.4								
	$6(D_3)$ internal	101.4								
	$4+2(C_s)$ surface	101.0								
	$4+2(C_1)^*$ surface	100.9								
	$6(C_2)$ internal	100.1								
	$3+3(C_1)$ surface	99.9								
	$3+3(C_3)$ surface	97.1								

[a]The BSSE-corrected energies are denoted with superscript ''B,'' while otherwise the energies are BSSE-uncorrected energies. All the energies are in kcal mol^{-1}. Some conformers (Most conformers for $n \leqslant 5$ and three conformers for $n=6$) were already reported by Combariza and Kestner using the same HF method with ours (see the text and refer to Ref. 14).

[b]HF calculation is represented by 6-31+G* basis sets and a full double-ζ basis sets of Mclean–Chandeler (Ref. 34) as parent functions to represent the fluoride anion.

[c]The free energy was corrected by $RT \ln 2 (=0.4$ kcal $mol^{-1})$ due to chirality.

The H–O–H bond angle is smaller than the free water monomer by about 2.86 deg, whereas one O–H length interacting with F^- ion has increased by almost 0.10 Å. In the case of the other O–H, the bond length increase from the isolated water structure is negligible (0.001 Å). A substantial effect of correlation has been observed on F–H length. In comparison to 1.49 Å at the HF level, this length is 1.39 Å at the MP2 level, and 1.41 Å at the BLYP level.

For the $F^-(H_2O)_2$ cluster, a bent $2(C_2)$ structure has the minimum energy. The linear $2(C_{2v})$ and $2(C_{2h})$ structures are very close in energy to the minimum energy structure. In BLYP calculation, the $2(C_{2v})$ is a transition state structure with one imaginary frequency, and it is only 0.2 kcal mol^{-1} above a local minimum energy structure $2(C_{2h})$. However, in MP2/6-311++G** calculation, $2(C_{2h})$ turns out to be a third-order saddle point and is 0.2 kcal mol^{-1} above the C_{2v} structure. The previous MP2 calculations by Xantheas *et al.*,[15] using the aug-cc-pVDZ basis set, has shown that $2(C_{2h})$ is a transition state. So, the status of this particular structure of the $F^-(H_2O)_2$ cluster is quite controversial. The energy differences between these structures are so small that they could be considered to be almost floppy. In such a situation, as was indicated by Schaefer and co-workers,[41] the inconsistencies between the results with different levels of calculation are not unusual. The fourth, high-energy, $2(C_{2v})$ structure was identified to be a third-order saddle point from frequency calculations and it lies ~10 kcal mol^{-1} above all the other low-energy structures. The ΔG for these structures indicate that two or three low-energy structures, *viz.*, $2(C_2)$, $2(C_{2h})$ [and $2(C_{2v})$], are almost degenerate, and thus they

TABLE II. Important bond lengths (r/Å) and bond angles (H–O–H/degree) for the low energy structures of $F^-(H_2O)_n$ ($n=1-6$) clusters.

		r(F–H_{near})			r(F–H_{far})	r(F–O)			r(O–H)[a]		(H–O–H)
n	Structure	MP2	BLYP	HF	MP2	MP2	BLYP	HF	MP2		MP2
1	$1(C_s)$ H-bonded	1.386	1.406	1.494	2.736	2.436	2.481	2.494	1.052	0.958	100.60
2	$2(C_2)$ bent	1.520	1.543	1.542	2.804	2.526	2.569	2.569	1.011	0.958	100.67
3	$3(C_3)$ surface	1.592	1.620	1.693	2.857	2.582	2.628	2.642	0.995	0.958	100.94
4	$4(C_1)$ internal	1.628	1.661	1.660	2.879	2.611	2.660	2.659	0.989	0.958	101.24
		1.712	1.751	1.742	2.827	2.663	2.708	2.705	0.982	0.962	99.64
		1.719	1.738	1.751	2.831	2.665	2.700	2.708	0.982	0.962	99.65
		1.714	1.741	1.739	2.831	2.661	2.705	2.700	0.983	0.962	99.86
	$3+1(C_s)$ trisolvated	1.555	1.585		2.895	2.550	2.598		1.000	0.958	102.33
		1.616	1.643		2.854	2.599	2.645		0.991	0.958	101.17
						3.853	3.903		0.969	0.969	101.14
	$4(C_{4h})$ planar	1.672	1.700		2.947	2.654	2.699		0.984	0.959	101.41
5	$3+2(C_1)$ surface	1.511	1.584	1.573	2.920	2.514	2.595	2.554	1.006	0.958	103.20
		1.553	1.716	1.647	2.874	2.545	2.704	2.610	1.000	0.959	102.24
		1.680	1.545	1.729	2.932	3.090	2.566	2.685	0.985	0.965	102.20
						3.853	3.745	3.981	0.971	0.969	103.12
						3.642	3.904	3.761	0.972	0.971	101.73
	$4+1(C_1)$ internal	1.779	1.809	1.810	2.869	2.727	2.765	2.740	0.976	0.962	99.60
		1.641	1.679	1.761	2.959	2.619	2.670	2.700	0.987	0.959	102.00
		1.606	1.638	1.686	2.930	2.593	2.640	2.648	0.991	0.959	102.34
		1.603	1.634	1.677	2.930	2.592	2.640	2.642	0.991	0.959	102.32
						3.988	3.984	4.032	0.969	0.968	101.09
	$5(C_1)$ internal[b]	1.769	1.821	1.847	2.910	2.718	2.770	2.769	0.978	0.963	99.98
6	$4+2(C_2)$ surface	1.597	1.631	1.690	2.932	2.576	2.628	2.646	0.992	0.959	102.53
		1.746	1.801	1.803	2.961	2.706	2.773	2.748	0.978	0.968	100.79
						3.543	3.625	3.666	0.970	0.972	102.21
	$4+2(C_1)$ internal	1.670	1.703	1.759	2.920	2.648	2.696	2.711	0.983	0.959	101.45
		1.689	1.643	1.719	2.866	2.647	2.641	2.668	0.984	0.962	100.93
		1.548	1.607	1.628	2.997	2.539	2.615	2.601	0.999	0.959	103.91
		1.713	1.777	1.778	2.977	2.684	2.759	2.733	0.980	0.966	102.24
						3.893	3.963	3.879	0.972	0.971	101.58
						3.955	3.843	4.034	0.969	0.970	102.78
	$6(S_6)$ internal	1.847		1.920	2.912	2.772		2.822	0.974	0.964	100.00

[a]The first column denotes the O–H length where the H is hydrogen bonded to fluorine, while the second column corresponds to the case when the hydrogen atoms are not hydrogen bonded to fluorine.
[b]Only average values are given.

might compete with each other to be the ground-state geometry. It is interesting to note that the 1.520 Å F–H distance in $2(C_2)$ is much longer than the corresponding distance of 1.386 Å in $1(C_2)$ (Table II).

The three structures considered for $F^-(H_2O)_3$ were $3(C_3)$, $3(C_{3h})$, and $2+1(C_s)$. The minimum energy structure was $3(C_3)$ in ΔE_e. The ZPE correction (ΔE_0), on the other hand, makes the minimum energy $3(C_{3h})$, which is otherwise a transition state in terms of ΔE_e. In terms of ΔG, $3(C_3)$ and $3(C_{3h})$ are the lowest energy conformers. This is in agreement with the results of Xantheas and Dunning.[15]

The structures of the $F^-(H_2O)_4$ cluster pose some interesting features. Combariza and Kestner[14] reported a pyramidal $4(C_1)$ internal structure to be the minimum energy structure. Bryce *et al.*,[18] from QM/MM studies, have observed that a trisolvated $3+1(C_s)$ planar-like (both surface-like and internal-like) structure was the most favored cluster arrangement. We have considered all such possibilities in our calculations. The BLYP results indicate that the $3+1(C_s)$ structure is more favored in ΔE_e and ΔE_0 than the internal $4(C_1)$ pyramidal structure, while the two structures are almost isoenergetic in ΔG. On the other hand, in the case of MP2 calculations, the $4(C_1)$ internal structure is slightly more stable in ΔE_e and ΔG than the $3+1(C_s)$ surface structure. It is likely that at 0 K the surface structures compete with the internal structures, while at 298 K the internal structures would be favored due to the entropic effect. The $4(C_{4h})$ planar structure, though a second-order saddle point, is almost as stable in ΔG as the $4(C_1)$ internal structure.

In the case of $F^-(H_2O)_5$ cluster, five possible structures have been considered. The prism $3+2(C_1)$ surface structure is the minimum energy geometry in ΔE_e, while the tetrasolvated $4+1(C_1)$ internal structure turns out to be the minimum energy geometry in ΔE_0 and ΔG (298 K and 1 atm), followed by the $5(C_1)$ internal structure.

A large number of structural possibilities has been considered for the $n=6$ cluster. These possibilities were mostly considered from our previous observations on the $(H_2O)_6^-$ clusters[28] as well as from the structures of $F^-(H_2O)_6$ considered by Combariza and Kestner.[14] The binding energies of the clusters presented in Table I at the HF level indicate that some of the conformers are of very high energy, and thus, only 6 conformers were studied for further analysis. Both the BLYP and MP2 energy calculations have indicated that the $4+2(C_2)$ surface structure is the minimum energy structure

in ΔE_0, and it is much lower in energy than other conformers. In ΔE_0, the $4+2(C_2)$ is again the minimum energy geometry, but it is almost isoenergetic to $4+2(C_1)$ internal structure. In terms of ΔG (at 298 K and 1 atm), the $4+2(C_1)$ internal structure is the lowest energy conformer, followed by the $4+2(D_2)$ internal structure, $5+1(C_1)$ internal structure, and $4+2(C_2)$ surface structure. Therefore, at 0 K the surface state $4+2(C_2)$ would be favored and it competes with the internal $4+2(C_1)$ structure, while at 298 K and 1 atm the internal $4+2(C_1)$ structure is favored, followed by the internal $4+2(D_2)$. The V-shaped $4+2(C_1)$ surface structure, which was assumed to be of lowest energy by Combariza and Kestner,[14] turns out to be second lowest in ΔE_e, but third lowest in ΔE_0, and a high-energy state in ΔG. The other two proposed structures are of much higher energies. It is to be further noted that with increasing cluster size of $F^-(H_2O)_n$, the water shell structures play an important role to stabilize the cluster structure.

The change of $F^-\cdots H$, O–H (H, hydrogen bonded to F), $F^-\cdots O$ lengths and H–O–H bond angle with increasing cluster size are presented in Fig. 3. The variations are presented for the lowest energy structures (in ΔE_e) for each cluster. They are usually n_1 type up to $n=4$. For $n=5$ and 6, they are (n_1+n_2) type. The $F^-\cdots H$ hydrogen bonding is strongest for the $n=1$ case, and with the increase of the cluster size the strength decreases. This is reflected in the trend of the $F^-\cdots H$ and $F^-\cdots O$ lengths in the clusters $n=1-4$. For $n=5$ and 6 clusters, the inclusion of a second hydration shell does not change the $F^-\cdots H/O$ interaction very much, and thus the $F^-\cdots H/O$ lengths are flattened out from $n=4-6$ clusters. The lowest energy n_1 structures for $n=5$ and 6 clusters, of course, show continuous increase of these lengths, as the increase of coordination number of F^- in the first hydration shell weakens the $F^-\cdots H$ bond strengths. The effect of $F^-\cdots H$ interaction is less pronounced in O–H length variation. In the $n=1$ cluster, the length increases with respect to free water. But, with increase of cluster size, the O–H length decreases due to weak $F^-\cdots H$ interactions, and the O–H lengths for $n=3-6$ clusters are more or less similar. As a result of these interactions, the H–O–H bond angle is always smaller than the free water, and its variations reflect the effect of such interactions in different clusters.

TABLE III. ΔH and ΔG values at 298 K for the $F^-(H_2O)_n$ $(n=1-6)$ clusters at the BLYP and MP2 levels.[a]

	BLYP		MP2		Expt.[b]	
n	$-\Delta H$	$-\Delta G$	$-\Delta H$	$-\Delta G$	$-\Delta H$	$-\Delta G$
1	29.29	22.73	27.98	21.42	23.30	18.1
2	48.98	36.51	47.83	35.28	42.5, 39.9	30.8, 29.1
3	64.99	44.13	64.80	43.89	57.8, 53.6	39.3, 36.7
4	76.75	46.75	78.10	48.09	71.7, 67.1	45.3, 42.2
5	89.03	49.42	91.45	52.04	84.0, 80.3	49.9, 46.2
6	100.26	50.01	104.34	54.07	94.9	53.4
	$-\Delta H^S$	$-\Delta G^S$	$-\Delta H^S$	$-\Delta G^S$	$-\Delta H^S$	$-\Delta G^S$
1	29.29	22.73	27.98	21.42	23.3	18.1
2	19.69	13.78	19.85	13.86	19.2, 16.6	12.6, 11.0
3	16.02	7.62	16.97	8.61	15.3, 13.7	8.5, 7.6
4	11.75	2.62	13.30	4.20	13.9, 13.5	6.0, 5.5
5	12.28	2.67	13.35	3.95	12.3, 13.2	4.6, 4.1
6	11.23	0.59	12.89	2.03	10.9	3.5

[a]All units are in kcal mol^{-1}. Superscript ''S'' denotes the successive interaction energy. The energies are presented with and without BSSE corrections. Mixing free energies are taken into account.
[b]Refs. 7 and 8.

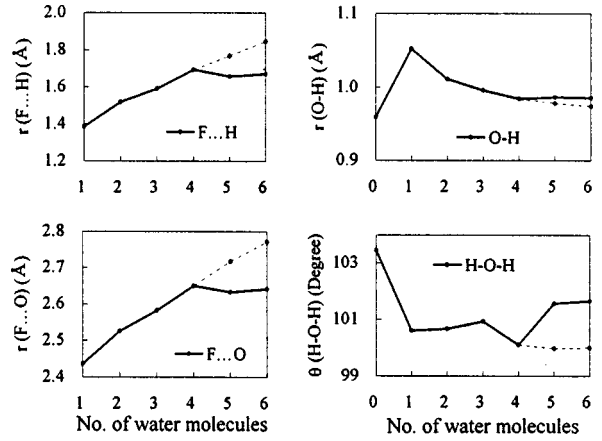

FIG. 3. Variation of the lengths $r(F\cdots H)$, $r(F\cdots O)$, and $r(O–H)$ and H–O–H angle $[\theta(H–O–H)]$ with increasing water molecules in clusters $F^-(H_2O)_n$. The parameters are chosen for the minimum energy (MP2) geometries of each cluster. The dotted lines indicate the values for the minimum energy n_1 cluster $(n_2=0)$ of $n=5$ and 6 clusters.

B. Thermodynamic quantities

Using the calculated thermodynamic data presented in Table I, we have calculated the ΔH and ΔG values, considering Boltzmann distribution of the low-energy structures of various cluster sizes. In calculating ΔG of the various low-energy structures, the free-energy lowering due to their mixing was taken into account. The results including the successive interaction energies (ΔH_s and ΔG_s) defined as $H_s(n)=H(n)-H(n-1)$, and $G_s(n)=G(n)-G(n-1)$, are presented in Table III. The table contains the values of the thermodynamic quantities using both BSSE-uncorrected and corrected energies obtained through MP2 and BLYP calculations. The plots of the predicted thermodynamic quantities with respect to the experimental values are presented in Fig. 4. The experimental energies of Arshadi *et al.*[8] were consistently 10%–20% underestimated than those of Hiraoka and co-workers,[7] in which the ΔG and ΔH for the first water solvation were not reported. So, as long as we use the experimental values of Arshadi *et al.*, the ΔG and ΔH for the first water solvation would be consistently larger than the plotted value for the experimental fit. Thus, the slope of the curve is important with increasing number of water molecules in the figure. The BSSE-uncorrected values are consistent with the experimental values, while the BSSE-corrected values are quite underestimated for $n \geqslant 4$. It is to be noted further that for a small number of water molecules, the BSSE-corrected values seem to be closer to the experimental values, while with increasing number of water molecules, the BSSE-uncorrected values need to be used. Nevertheless, the

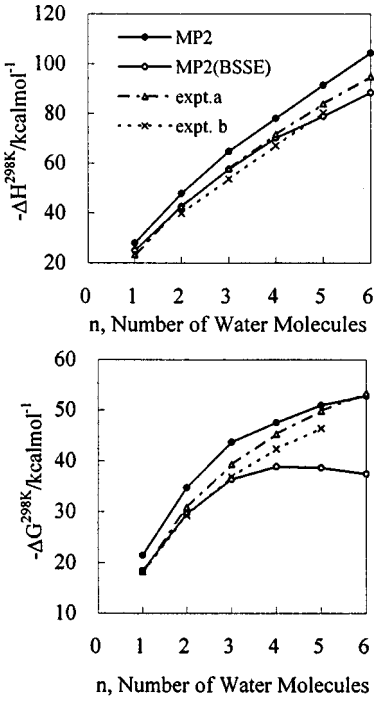

FIG. 4. Plots of experimental and calculated (MP2) ΔH and ΔG values of $F^-(H_2O)_n$ clusters with increasing $n(n=1-6)$.

overall good agreement surely comes from the BSSE-uncorrected values. Thus, our discussion is based only on these values.

The agreement of the MP2 results is better for both the ΔH and ΔG calculations than the BLYP results. In earlier theoretical studies, the experimental thermodynamic parameters were only compared with those derived from the minimum energy geometry of the clusters. In our present study, we have found that the energetics of the $F^-(H_2O)_n$ clusters with different sizes predict the probability of more than one geometry. For $n \geqslant 4$, the number of probable geometries was found to be quite appreciable. The agreement of ΔH or ΔG values with the experimental results actually supports the presence of several low-energy clusters for $F^-(H_2O)_n$ $(n \geqslant 4)$. The probabilistic configurational distribution is important in evaluating free energies and enthalpies. Since several configurations are somewhat isoenergetic, more than one geometry was considered. Moreover, transition states other than the minimum energy structures were also taken into account. Because of the entropic effect, such structures could also be stable. In this way, a high anharmonicity effect was also taken into account. Moreover, the very low-frequency modes giving unrealistic overestimation of the vibrational entropies in this case are replaced by the rotational degrees of freedom corresponding to the maximum rotational entropy of a water monomer. In MD simulations, often the multiminima effect has been stressed. Though this is true, the potentials employed are not always realistic. Sometimes the order of structural stability changes, and although the entropic effect could be taken into account, they are often based on nonexact potential energy surface. Thus, this *ab initio* approach would be more reliable for small cluster systems having several discrete low-energy conformers.

C. Analysis of many-body interaction energies

Table IV contains the $F^-\cdots H_2O$ (F–W) and $H_2O\cdots H_2O$ (W–W or W_2) interaction terms for a number of representative low-lying conformers of $F^-(H_2O)_n$ clusters $(n=2-6)$. The analysis of such interaction terms usually gives a better understanding of the nature of interactions operative in weak clusters.[24,38] For $F^-(H_2O)_n$ clusters, Xantheas *et al.* have made a detailed analysis for $n=1-3$.[15] In our present analyses, interactions are studied up to four-body terms without any BSSE corrections for $n=2-6$ clusters. It is interesting to note that although the stabilization energies of the low-lying structures mostly come from the F–W and W–W two-body interaction terms, the repulsive three-body and, in some cases, attractive four-body terms are gaining importance to account for the stability order of the low-lying energy structures of higher clusters. This is particularly true for the $n=5$ and $n=6$ cases. It is to be noted further that in $n=5$ and 6 clusters, although the water deformation energies due to the presence of the F^- ion are important to account for the total interaction energy of the different low-lying structures, they are not playing a decisive role to account for their stability order. The contribution of five- and six-body terms for $n=5$ and five-, six-, and seven-body terms for $n=6$ clusters is not presented here, but could be easily calculated using the total MP2 binding energies of the respective clusters, and the interaction energies presented in Table IV. They are usually very small, but sometimes could be important to account for the small energy difference between the various low-lying energy structures, especially, in the $n=5$ case. Table IV further contains the correlation energies of the different low-lying structures of $n=2-6$ clusters. It could be seen from these results that if there is no second hydration layer in the clusters, it is usually 10% of the total binding energy. With the addition of a second solvation layer, it is 14%–15% of the total binding energy. Since the overall correlation is more than 10% of the total binding energies, it reflects the need for the use of higher correlated methods in such structure calculations.

D. Ionization potentials

The use of ionization potentials (IPs), especially the ionization potential shifts, has proven useful in elucidating the preferred surface or interior structures in cases where the energy differences are very small. According to Combariza, Kestner, and Jortner,[21] we have considered integral and differential shifts. Representing the vertical ionization potentials of F^- and $F^-(H_2O)_n$ cluster as $IP_v(F^-)$ and $IP_v[F^-(H_2O)_n]$, the integral shift $dIP_v(n)$ and the differential shifts $DIP_v(n)$ for the nth $F^-(H_2O)_n$ cluster are represented as $dIP_v(n)=IP_v[F^-(H_2O)_n]-IP_v(F^-)$ and $DIP_v(n)=IP_v[F^-(H_2O)_n]-IP_v[F^-(H_2O)_{n-1}]$, respectively.

The values for IP_v, dIP_v, and DIP_v obtained from Koopmans' theorem as the MP2 calculation, are presented in Table V, which will be useful information for experimentalists. It can be seen from the table that the integral shifts increase monotonically up to $n=3$. For $n=4$, the $dIP_v(4)$ for both the internal and surface states flattens out. It is to be noted further that the differences of $dIP_v(n)$ and $DIP_v(n)$ for

TABLE IV. Decomposition of the interaction energies (MP2/6-311++G**) for the low-energy clusters of the $F^-(H_2O)_n$ ($n=2-6$) systems.[a]

n	Structure	deformation	2-body total (F–W, W_2)	3-body total (F–W_2, W_3)	4-body total (F–W_3, W_4)	Interaction energy	E_{corr}
2	$2(C_2)$	2.97	−55.88 (−56.79, 0.91)	3.75 (3.75, 0)		−49.16	−5.12
	$2(C_{2h})$	2.72	−55.44 (−56.34, 0.90)	4.08 (4.08, 0)		48.64	−4.20
3	$3(C_3)$	2.35	−78.62 (−81.14, 2.52)	9.06 (9.30, −0.24)	−0.22(−0.22, 0)	−67.43	−6.43
	$2+1(C_s)$	3.71	−74.92 (−69.40, −5.52)	3.87 (2.98, 0.88)	0.44(0.44, 0)	−66.90	−8.95
4	$4(C_1)$	1.94	−100.03 (−101.39, 1.37)	15.20 (16.14, −0.94)	−0.73(−0.73, 0.00)	−83.62	−8.52
	$3+1(C_s)$	2.62	−95.62 (−92.43, −3.19)	9.46 (8.88, 0.58)	−0.04(−0.04, 0.00)	−83.58	−9.91
5	$3+2(C_1)$	2.87	−116.65 (−98.60, −14.38)	11.18 (11.87, −0.68)	−0.91(−0.84,−0.07)	−99.84	−14.45
	$4+1(C_1)$	2.09	−112.98 (−113.71, −2.94)	16.50 (16.55, −0.05)	−0.90(−0.85,−0.05)	−98.96	−11.35
	$5(C_1)$	1.79	−119.02 (−121.08, 2.05)	21.43 (23.73, −2.30)	−1.72(−1.63,−0.09)	−97.52	−11.00
6	$4+2(C_2)$	2.14	−135.10 (−11.9.65, −15.45)	18.85 (22.08, −3.22)	−1.80(−2.13, 0.33)	−115.91	−16.57
	$4+2(C_1)$	2.36	−132.69 (−115.63, −17.06)	17.43 (20.14, −2.71)	−2.14(−2.08,−0.05)	−115.04	−17.38
	$4+2(C_1)$	2.25	−132.58 (−118.85, −13.72)	17.65 (18.76, −1.11)	−1.92(−1.65,−0.26)	−114.60	−15.72
	$6(S_6)$	1.61	−135.24 (−138.29, 3.05)	27.83 (31.54, −3.71)	−1.81(−2.13, 0.31)	−107.61	−11.78

[a]W denotes a water monomer and W_i ($i=2-4$) denotes higher-order water many-body terms.
[b]Considering E_i to be the energy of a deformed water molecules in the cluster and E_w the energy of the gas phase water molecules, the deformation energy is calculated as $E_0=\Sigma_{i=1}^{n}E_i-nE_w$; n, the number of water molecules in the cluster.

the internal or surface states are very small. This observation is quite similar to that of Combariza and Kestner.[28]

We have also considered the energy band gap or the ionization potential at the situation of the CTTS system (E_{CTTS}).[10] An empirical estimate of this energy is obtained by subtracting the energy of the system for an excess electron in the frozen water cluster with the F^- ion ejected from the energy for the corresponding neutral frozen water system. This is also listed in Table V, together with polarizability values (α). The more precise definition of CTTS energy indicates that it is an electronic transition related to the transfer of charges from the fluoride to the water, and the energy would be less than the IP of the corresponding anion water system.[10] Keeping this definition of E_{CTTS} in mind, we have further explored the vertically excited states of the different MP2-optimized low-energy clusters of $F^-(H_2O)_n$ ($n=2-6$) using time-dependent discrete Fourier transform (DFT) method[42] of GAUSSIAN-98 program suite.[40] This method was particularly chosen as it usually gives more accurate estimation of the vertical transition energy with respect to the normal first-order configuration interaction (FOCI) calculations. The results are included in Table V along with the empirical CTTS energies. The results maintain a similar trend to the empirically calculated E_{CTTS} values for different clusters. We have further calibrated this approach by calculating the experimentally observed E_{CTTS} values of $I^-(H_2O)_2$ and $I^-(H_2O)_4$ clusters.[10] Our calculated values of vertical transition energies for the S_1 states for the two clusters are 4.036 and 4.437 eV, respectively, as compared to their respective experimental E_{CTTS} values of 3.95 and 4.5 eV. In view of the calculated I^- charges of the $S_0(-0.82)$ and $S_1(-0.58)$ states of the $I^-(H_2O)_2$ cluster, this S_1 state could be assigned

TABLE V. NBO charge of $F^-(q_F)$, mean polarizability (α), vertical ionization potential (IP), their integral ($d\mathrm{IP}_v$), differential ($D\mathrm{IP}_v$) shifts, and charge-transfer-to-solvent energy (E_{CTTS}) for the various low energy geometries of $F^-(H_2O)_n$ ($n=1-6$) clusters at the MP2 level.[a]

n	Structure	q_F	α	$\Delta\alpha$	IP_v (eV)	$d\mathrm{IP}_v$ (eV)	$D\mathrm{IP}_v$ (eV)	E_{CTTS}[b]
1	$1(C_s)$ H-bonded	−0.87	19.62	6.61	5.54 (6.43)	2.20 (3.09)	2.20 (3.09)	5.52
2	$2(C_2)$ bent	−0.85	29.60	8.62	6.25 (7.67)	2.91 (4.33)	0.71 (1.24)	5.93 (4.59)
	$2(C_{2h})$ linear	−0.86	29.46	8.48	6.20 (7.60)	2.86 (4.26)	0.67 (1.17)	5.88
3	$3(C_3)$ surface	−0.83	38.53	9.60	7.21 (8.56)	3.87 (5.22)	0.96 (0.89)	6.39 (5.17)
	$2+1(C_s)$ surface	−0.82	39.99	11.06	6.89 (8.56)	3.55 (5.22)	0.64 (0.89)	6.17
4	$4(C_1)$ internal	−0.85	48.74	11.85	7.64 (8.99)	4.30 (5.65)	0.43 (0.43)	6.66 (5.70)
	$3+1(C_s)$ trisolvated	−0.82	49.33	12.44	7.31 (8.80)	3.97 (5.46)	0.10 (0.23)	6.48
	$4(C_4)$ surface	−0.84	48.92	12.03	7.27 (9.17)	3.93 (5.83)	0.06 (0.61)	6.70
5	$3+2(C_1)$ surface	−0.81	59.94	15.09	7.51 (9.03)	4.17 (5.69)	0.20 (0.23)	6.59
	$4+1(C_1)$ internal	−0.83	58.56	13.71	7.57 (9.07)	4.23 (5.73)	0.26 (0.28)	6.81 (5.23)
	$5(C_1)$ internal	−0.85	58.42	13.57	8.15 (9.28)	4.81 (5.94)	0.84 (0.48)	6.91
	$5(C_1)$* internal	−0.85	58.14	13.28	7.86 (9.34)	4.52 (6.00)	0.55 (0.54)	6.88
6	$4+2(C_2)$ surface	−0.83	69.77	16.96	8.33 (9.38)	4.99 (6.04)	0.76 (0.31)	6.83 (5.46)
	$4+2(C_1)$ surface	−0.83	69.53	16.72	8.22 (9.31)	4.88 (5.97)	0.65 (0.24)	6.80
	$4+2(C_1)$ internal	−0.82	69.01	16.20	8.45 (9.42)	5.11 (6.08)	0.88 (0.35)	6.85
	$3+3(C_3)$ surface	−0.81	70.19	17.38	7.76 (9.27)	4.42 (5.93)	0.19 (0.20)	6.66
	$4+2(D_2)$ internal	−0.82	68.96	16.15	7.79 (9.41)	4.45 (6.07)	0.23 (0.34)	6.88

[a]IP_v, $d\mathrm{IP}_v$, $D\mathrm{IP}_v$ were obtained by the energy difference of the ionic and neutral species keeping the geometry unchanged, while their values in parentheses were obtained using Koopman's theorem. Polarizabilities are in a.u., E_{CTTS} in eV.
[b]Values within parentheses are the vertical transition energy to the S_1 state for the corresponding MP2 optimized geometry.

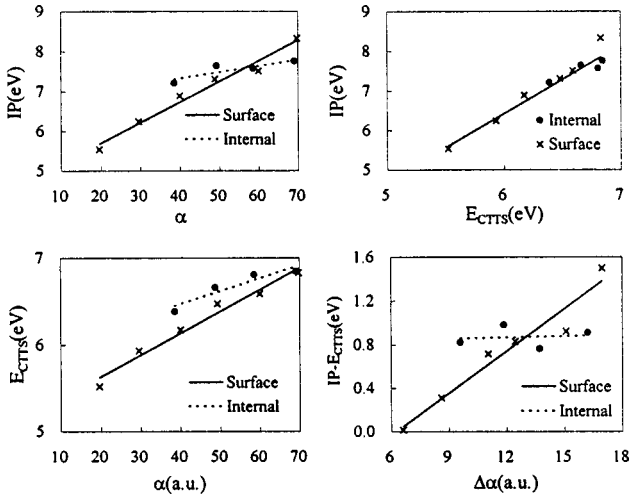

FIG. 5. Plots of IP vs α, E_{CTTS} vs α, IP vs E_{CTTS}, and (IP$-E_{CTTS}$) vs $\Delta\alpha$ for the surface and internal lowest energy structures of $F^-(H_2O)_n$, $n=1-6$.

to be the CTTS state of this cluster. For $F^-(H_2O)_n$ clusters, on the other hand, the amount of charge transfer to the CTTS is quite small (~0.04 e), as is quite expected from the very high electronegativity of fluorine.

Figure 5 indicates the linear relationships of α with IP and empirically calculated E_{CTTS} and of IP with E_{CTTS}. The plot of the difference of IP and E_{CTTS} against $\Delta\alpha$ $(=\alpha[F^-(H_2O)_n]-n\alpha[H_2O]-\alpha[F^-])$ shows a similar trend. However, the surface structures show steep increase of IP and E_{CTTS} with increasing α, while the internal structures show partial saturated polarization effects with little increase, particularly for the value of IP-E_{CTTS}. Although the E_{CTTS} of different aqua anions were found to be linearly related to their respective IPs,[10] such types of relationships with varying cluster sizes for the same aqua anions have not been reported so far.

E. Vibrational frequencies and IR spectra

The BLYP OH stretching harmonic vibrational spectra for the low-energy geometries of $F^-(H_2O)_n$ $(n=1-6)$ clusters are presented in Table VI and Fig. 6. The results include only the different O–H stretching frequencies. The O–H stretching frequencies in fluoride–water clusters could be classified as (i) nonbonded free $[\omega(O-H_n)]$, (ii) hydrogen bonded to another water $[\omega(O-H_{bw})]$, and (iii) hydrogen bonded to the fluoride atom $[\omega(O-H_f)]$. Apart from these three classes, a mixed type of O–H frequencies were observed in the $4+2(C_2)$ surface structure for the $n=6$ cluster. These O–H frequencies are different from the other three classes because of the influence of both fluoride and adjacent water molecules on the hydrogen atoms. This effect was observed due to special structural disposition of the $4+2(C_2)$ structure of $F^-(H_2O)_6$. It has been found that, for the elongation of the OH bonds due to hydrogen bonding, the O–H frequencies show redshift with respect to the average of the symmetric and asymmetric stretches of water (3725 cm^{-1}). The magnitude of the shift follows the same trend as the elongation of the OH length, i.e., $\Delta\omega(O-H_n)<\Delta\omega(\text{mixed})<\Delta\omega(O-H_{bw})<\Delta\omega(O-H_f)$. However, $\Delta\omega$(mixed) was classified into $\Delta\omega(O-H_b)$ and $\Delta\omega(O-H_{bw})$, for convenience.

In the case of $n=1$ cluster, although the free O–H length remains almost unchanged with respect to the free water, the hydrogen-bonded O–H length with respect to the F^- ion is elongated considerably. This results in substantial redshift in the $\omega(O-H_f)$ with respect to the free water, whereas there is practically no shift in the nonhydrogen-bonded, free O–H stretching frequency $[\omega(O-H_n)]$. In the case of $n=2$ cluster, the trend of O–H stretching frequencies is more or less similar to the $n=1$ case. The only difference is that the redshift from the free water O–H stretching frequencies has drastically reduced. This indicates that the $F^-\cdots H_2O$ interaction has become weaker with respect to the $n=1$ case. This situation is quite obvious from the $F^-\cdots H$ distances (Table II). There is a trend of continuous reduction in the redshift of $(O-H_f)$ type frequency as the cluster size increases with a few exceptions in higher clusters where the $F^-\cdots H$ hydrogen bond is stronger with respect to the other $F^-\cdots H$ hydrogen bonds. This is due to the special structural arrangement of the cluster geometries, but on the average there is a reduction in $\omega(O-H_f)$ redshift. The redshifts (150–330 cm^{-1}) for type (ii) frequencies, that is, the O–H frequencies where the hydrogen is bonded to another water $[\omega(O-H_{bw})]$, are much less dependent on n. The redshifts in $O-H_{bw}$ frequencies of $4+1(C_1)$ is less than the $3+2(C_1)$ surface structure of $n=5$ cluster, indicating much stronger water–water interaction in the latter case. It is interesting to note that the stabilization of these two structures is due to dominance of two different types of interactions. In the case of $3+2(C_1)$ surface structure, apart from the $F^-\cdots H_2O$ interaction, the other countable dominant stabilizing force is $H_2O\cdots H_2O$ interaction, whereas in the case of tetrasolvated cluster $4+1(C_1)$, the dominating interaction is $F^-\cdots H_2O$ interaction. This is clearly reflected in the O–H stretching frequency values. In case of $5(C_1)$, all the water molecules are directly attached to the F^- ion and the $F^-\cdots H_2O$ interaction is the governing force for the stabilization of this cluster. The redshift in the O–H stretching frequencies are minimum in this cluster with respect to the other two $n=5$ clusters. The $4+2(C_2)$ of the $n=6$ cluster is a surface structure and it has typical O–H stretching frequencies which are not observed in other clusters. It arises from the interaction of the O–H bond with both F^- and other water molecules, and we have termed it as ω(mixed). The redshift of these frequencies from the average O–H stretching frequency of free water indicates that it is of intermediate strength with respect to the $(O-H_f)$ and $(O-H_{bw})$ frequencies, and thus these interactions are quite significant for the stabilization of this particular type of structure. The frequency values for other $n=6$ cluster indicate that their stabilization is mostly contributed by $F^-\cdots H_2O$ and $H_2O\cdots H_2O$ interactions.

The hydrogen of the O–H bonds, which is not interacting with anything, are considered as free, and the corresponding O–H frequencies are termed as free $(O-H_n)$. These frequencies, showing a small shift with respect to the O–H frequency of free water, have very weak intensities, thus these peaks are hardly seen in Fig. 6. In recent experi-

TABLE VI. Harmonic vibrational frequencies of O–H stretchings of the $F^-(H_2O)_n$ ($n=1-6$) clusters at the BLYP/6-311++G** level of calculations. Shifts (cm^{-1}) in the intermolecular harmonic frequencies of O–H stretchings of water are also included.

n	Structure	O–H stretching frequencies (cm^{-1})[a] $\omega(O-H_f)$[b]			$\omega(O-H_{bw})$[b]						$\omega(O-H_n)$[b]			
1	$1(C_s)$	2073									3721			
		(−1652)									(−4)			
2	$2(C_2)$	2652	2820								3728	3729		
		(−1072)	(−904)								(3)	(4)		
	$2(C_{2h})$	2691	2868								3734	3734		
		(−1034)	(−857)								(9)	(9)		
3	$3(C_3)$	2966	2966	3116							3731	3731	3732	
		(−759)	(−759)	(−609)							(6)	(6)	(7)	
4	$3+1(C_s)$	2864	2954	3130		3474	3514				3734	3736	3737	
		(−860)	(−771)	(−595)		(−251)	(−211)				(9)	(11)	(12)	
	$4(C_1)$	3133	3220	3230	3339						3665	3670	3680	3735
		(−591)	(−504)	(−494)	(−385)						(−59)	(−55)	(−44)	(10)
5	$3+2(C_1)$	2773	2937	3223		3398	3416	3449	3491	3570	3730	3737		
		(−952)	(−788)	(−501)		(−327)	(−309)	(−275)	(−233)	(−155)	(6)	(12)		
	$4+1(C_1)$	3043	3103	3204	3403	3488	3534				3671	3734	3735	3737
		(−682)	(−622)	(−521)	(−322)	(−236)	(−191)				(−53)	(9)	(10)	(12)
	$5(C_1)$	3203	3324	3365	3412	3469					3605	3610		3627
		(−522)	(−401)	(−360)	(−313)	(−256)					(−120)	(−115)		(−98)
											3633	3735		
											(−92)	(10)		
6	$4+2(C_2)$	3025	3109	3310	3363	3400	3416	3469	3485	3496	3500	3732	3733	
		(−700)	(−616)	(−415)	(−362)	(−325)	(−308)	(−256)	(−240)	(−229)	(−224)	(8)	(9)	
	$4+2(C_1)$	2993	3105	3251	3350	3410	3433	3469	3497	3539		3731	3735	3739
		(−731)	(−620)	(−474)	(−374)	(−315)	(−291)	(−256)	(−228)	(−185)		(6)	(10)	(15)
	$4+2(D_2)$	3142	3146	3150	3298	3497	3498	3540	3544			3731	3731	3731	3733
		(−582)	(−578)	(−575)	(−427)	(−226)	(−227)	(−185)	(−181)			(6)	(6)	(6)	(8)

[a]Shifts for each frequency are presented within parentheses with sign. The negative/positive signs indicate red/blue shifts. The shifts are computed with respect to average symmetric and asymmetric stretches of water (3725 cm^{-1}, in BLYP calculation).
[b]Subscripts *f*, *bw*, and *n*, are used to indicate, bonded to F, bonded to another water, and nonbonded free hydrogen atoms, respectively.

mental works, Johnson *et al.*[4,43] and Cabracos *et al.*[44] have observed the vibrational spectra of X^-H_2O (X=F, Cl, Br, and I) clusters. The paper by Cabarcos *et al.*[44] on the vibrational spectra of $F^-(H_2O)_n$ ($n=3-5$), especially the $n=5$ case, merits further discussion. The experimental redshifts in O–H stretching frequencies for $n=5$ cluster are −567, −321, −165 (all ionic), and −9 (free O–H) cm^{-1}. The authors have further calculated explicitly the conformational aspects and vibrational spectra of the clusters at the MP2 level using the aug-cc-pVDZ basis set. For the $n=5$ cluster, they have concluded that a $4+1(3)$ arrangement of water molecules around the F^- ion is the global minimum. This is energetically followed by a ''pyramid-like'' 4-1 and a $4+1(2)$ arrangements. The numbers within parentheses indicate the number of hydrogen bonds formed between the water molecules in the first hydration shell and the lone water molecule in the second hydration shell. The higher energy 4-1 pyramidal structure was found to reproduce the experimental spectra more closely than the other conformers. In our calculation, the 4-1 pyramidal structure could be identified as a $5(C_1)$ structure. It is the third-lowest energy geometry in our calculation. Consideration of the explicit entropic effect stabilizes it further and it turns out to be the second-lowest energy structure with respect to ΔG values (Table I). It can be seen from Table VI that this structure bears the minimum redshift in the O–H stretching frequencies and resembles the experimental as well as the calculated values more closely than the other two conformers.

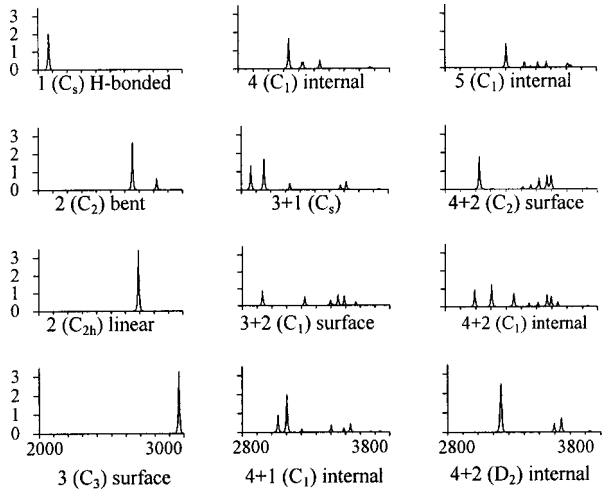

FIG. 6. BLYP/6-31++G**-predicted IR spectra of the O–H stretching frequencies for selected low-energy structures of $F^-(H_2O)_n$, $n=1-6$.

IV. CONCLUDING REMARKS

We have examined various structures of $F^-(H_2O)_n$, $n=1-6$ clusters, using *ab initio* calculations. The most reliable results presented here are based on MP2/6-311++G** calculations. The lowest energy structures for $n=1-6$ are predicted to be $1(C_s)$, $2(C_2)$, $3(C_{3h})$ [or $3(C_3)$], $4(C_1)$ [or

$3+1(C_s)]$, $3+2(C_1)$, $4+2(C_2)$ [or $4+2(C_1)$] at 0 K, and $1(C_s)$, $2(C_2)$, $3(C_3)$, $4(C_1)$, $4+1(C_1)$, and $4+2(C_1)$ at 298 K. For $n=5$, the internal structure is favored at both 0 and 298 K. For $n=4$ at 0 K, $4(C_1)$ and $3+1(C_s)$ compete with each other, whereas for $n=6$, $4+2(C_1)$ internal and $4+2(C_2)$ surface structures are close candidates for minimum energy geometry. On the other hand, the entropic effect favors the internal structures at higher temperature. For $n=4$, at 298 K the most favorable structures are not one, but a few conformers could coexist. Thus, configuration mixing entropy was considered in evaluating the free energies. The predicted ΔH and ΔG values calculated in this way, for $n=1-6$, are in good agreement with experiment. This indicates that our results are reliable, though further accurate calculations are desirable. Results of many-body interactions presented here would be of better help to understand the nature of interactions and to simulate the more realistic potential parameters. In addition, our results for IP, E_{CTTS} and vibrational spectral characteristics $(n=6)$ of these clusters are so far not available experimentally, and will be useful for further experimental investigations.

ACKNOWLEDGMENT

This work was supported by Creative Research Initiatives of Korean Ministry of Science and Technology. Calculations were performed using Cray T3E at SERI, Korea.

[1] H. Haberland, *Cluster of Atoms and Molecules* (Springer Series in Chemical Physics, Springer, Berlin, 1994).
[2] G. Markovich, S. Pollack, R. Giniger, and O. Cheshnovsky, J. Chem. Phys. **95**, 9416 (1991); *ibid.* **101**, 9344 (1994).
[3] M. Okumura, L. I. Yeh, J. D. Myers, and Y. T. Lee, J. Phys. Chem. **94**, 3416 (1989); Y. Cao, J. H. Choi, B.-M. Hass, M. S. Johnson, and M. Okumura, J. Chem. Phys. **99**, 9307 (1993); J. H. Choi, K. T. Kuwata, B. M. Hass, Y. Cao, M. S. Johnson, and M. Okumura, *ibid.* **100**, 7153 (1994); M. S. Johnson, K. T. Kuwata, C.-K. Wong, and M. Okumura, Chem. Phys. Lett. **260**, 551 (1996); J.-H. Choi, K. T. Kuwata, Y.-B. Cao, and M. Okumura, J. Phys. Chem. A **102**, 503 (1998).
[4] P. Ayotte, C. G. Bailey, and M. A. Johnson, J. Phys. Chem. B **102**, 3067 (1998); C. G. Bailey, J. Kim, C. E. H. Dessent, and M. A. Johnson, Chem. Phys. Lett. **269**, 122 (1997).
[5] C. Bassmann, U. Boesl, D. Yang, G. Drechsler, and E. W. Schlag, Int. J. Mass Spectrom. Ion Processes **153**, 159 (1996).
[6] P. Kebarle, M. Arshadi, and J. Scarborough, J. Chem. Phys. **49**, 817 (1968); P. Jayaweera, A. T. Blades, M. G. Ikonomou, and P. Kebarle, J. Am. Chem. Soc. **112**, 2452 (1990); A. T. Blades, P. Jayaweera, M. G. Ikonomou and P. Kebarle, J. Chem. Phys. **92**, 5900 (1990).
[7] M. Arshadi, R. Yamadgni, and P. Kebarle, J. Phys. Chem. **74**, 1475 (1970).
[8] K. Hiraoka, S. Mizuse, and S. Yamabe, J. Phys. Chem. **92**, 3943 (1988).
[9] A. N. Castleman, Jr. and M. G. Brown, J. Phys. Chem. **100**, 12911 (1996); X. Yang and A. W. Castleman, Jr., *ibid.* **94**, 8500 (1990).
[10] D. Serxner, C. E. H. Dessent, and M. A. Johnson, J. Chem. Phys. **105**, 7231 (1996); N. Takahashi, K. Sakai, H. Tanida, and I. Watanabe, Chem. Phys. Lett. **183**, 246 (1995).
[11] H. Kistenmacher, H. Popkie, and E. Clementi, J. Chem. Phys. **58**, 5627 (1973).
[12] B. F. Yates, H. F. Schaefer III, T. J. Lee, and J. E. Rice, J. Am. Chem. Soc. **110**, 6327 (1988).
[13] J. E. Combariza, N. R. Kestner, and J. Jortner, J. Chem. Phys. **100**, 2851 (1994); Chem. Phys. Lett. **203**, 423 (1993); G. Makov and A. Nitzan, J. Phys. Chem. **98**, 3459 (1994).
[14] J. E. Combariza and N. R. Kestner, J. Phys. Chem. **98**, 3513 (1994).
[15] S. S. Xantheas and T. H. Duning, Jr., J. Phys. Chem. **98**, 13489 (1994).
[16] S. S. Xantheas, J. Chem. Phys. **100**, 7523 (1994); J. Phys. Chem. **100**, 9703 (1996).
[17] S. S. Xantheas and L. X. Dang, J. Phys. Chem. **100**, 3989 (1996).
[18] R. A. Bryce, M. A. Vincent, N. O. Malcom, I. H. Hiller, and N. A. Burton, J. Chem. Phys. **109**, 3077 (1998).
[19] L. Perera and M. L. Berkowitz, J. Chem. Phys. **95**, 1954 (1991); *ibid.* **99**, 4222 (1993); *ibid.* **100**, 3085 (1994); L. S. Sremaniak, L. Perera, and M. L. Berkowitz, Chem. Phys. Lett. **218**, 377 (1994).
[20] I.-C. Yeh, L. Perera, and M. L. Berkowitz, Chem. Phys. Lett. **264**, 31 (1997).
[21] L. X. Dang and B. C. Garrett, J. Chem. Phys. **99**, 2972 (1993); H. Gai, G. K. Schenter, L. X. Dang, and B. C. Garrett, *ibid.* **105**, 8835 (1996).
[22] W. L. Jorgensen and D. L. Severance, J. Chem. Phys. **99**, 4233 (1993); J. Gao, D. S. Garner and W. L. Jorgensen, J. Am. Chem. Soc. **108**, 4784 (1986).
[23] T. N. Truong and E. V. Stefanovich, Chem. Phys. **31**, 218 (1997).
[24] J. Kim, S. Lee, S. J. Cho, B. J. Mhin, and K. S. Kim, J. Chem. Phys. **102**, 839 (1995).
[25] M. M. Probst, Chem. Phys. Lett. **137**, 229 (1987); C. W. Bauschlicher, S. R. Langhoff, H. Partridge, J. E. Rice, and A. Kormornicki, J. Chem. Phys. **95**, 5142 (1991); B. J. Mhin, J. Kim, and K. S. Kim, Chem. Phys. Lett. **216**, 305 (1993); K. S. Kim, S. Lee, B. J. Mhin, S. J. Cho, and J. Kim, *ibid.* **216**, 309 (1993); J. Kim, J. K. Park, and K. S. Kim, J. Phys. Chem. **100**, 14329 (1996).
[26] E. D. Glendening and D. Feller, J. Phys. Chem. **99**, 3060 (1995); D. Feller, E. D. Glendening, D. E. Woon, and M. W. Feyereisen, J. Chem. Phys. **103**, 3526 (1995); E. S. Marcos, J. M. Martinez, and R. R. Pappalardo, *ibid.* **105**, 5968 (1996); A. Bagno, V. Conte, F. D. Furia, and S. Moro, J. Phys. Chem. A **101**, 4637 (1997).
[27] M. Armbruster, H. Haberland, and H.-G. Schindler, Phys. Rev. Lett. **47**, 323 (1981); H. Haberland, C. Ludewigt, H.-G. Schindler, and D. R. Worsnop, J. Chem. Phys. **81**, 3742 (1984); L. A. Posey and M. A. Johnson, *ibid.* **89**, 4807 (1988); L. A. Posey, P. J. Capagnola, M. A. Johnson, G. H. Lee, J. G. Eaton, and K. H. Bowen, *ibid.* **91**, 6536 (1989); J. V. Coe, G. H. Lee, J. G. Eaton, S. T. Arnold, H. W. Sarkas, K. H. Bowen, C. Ludewigt, H. Haberland, and D. R. Worsnop, *ibid.* **92**, 3980 (1990); C. Desfrancois, N. Khelifa, A. Lisfi, J. P. Schermann, J. G. Eaton, and K. H. Bowen, *ibid.* **95**, 7760 (1991); P. J. Campagnola, D. J. Lavrich, M. J. DeLuca, and M. A. Johnson, *ibid.* **94**, 5240 (1991); P. J. Campagnola, L. A. Posey, and M. A. Johnson, *ibid.* **95**, 7998 (1991); S. T. Arnold, R. A. Morris, A. A. Viggiano, and M. A. Johnson, J. Phys. Chem. **100**, 2900 (1996); P. Ayotte and M. A. Johnson, J. Chem. Phys. **106**, 811 (1997); P. Ayotte, C. G. Bailey, J. Kim, and M. A. Johnson, *ibid.* **108**, 444 (1998).
[28] B. K. Rao and N. R. Kestner, J. Chem. Phys. **80**, 1587 (1984); N. R. Kestner and J. Jortner, J. Phys. Chem. **88**, 3818 (1984); R. N. Barnett, U. Landman, C. L. Cleveland, and J. Jortner, Phys. Rev. Lett. **59**, 811 (1987); J. Chem. Phys. **88**, 4429 (1988); R. N. Barnett, U. Landman, and A. Nitzan, Phys. Rev. Lett. **62**, 106 (1989); J. Kim, J. M. Park, K. S. Oh, J. Y. Lee, S. Lee, and K. S. Kim, J. Chem. Phys. **106**, 10207 (1997).
[29] K. S. Kim, I. Park, S. Lee, K. Cho, J. Y. Lee, J. Kim, and J. D. Joannopoutos, Phys. Rev. Lett. **76**, 956 (1996); S. Lee, S. J. Lee, J. Y. Lee, J. Kim, K. S. Kim, I. Park, K. Cho, and J. D. Joannopoulos, Chem. Phys. Lett. **234**, 128 (1996); K. S. Kim, S. Lee, J. Kim, and J. Y. Lee, J. Am. Chem. Soc. **119**, 9329 (1997); S. Lee, J. Kim, S. J. Lee, and K. S. Kim, Phys. Rev. Lett. **79**, 2038 (1997).
[30] A. D. Becke, Phys. Rev. A **38**, 3098 (1988); C. Lee, W. Yang, and R. G. Parr, Phys. Rev. B **37**, 785 (1988).
[31] A. D. Mclean and G. S. Chandler, J. Chem. Phys. **72**, 5639 (1980).
[32] S. F. Boys and F. Bernardi, Mol. Phys. **19**, 553 (1970).
[33] K. S. Kim, B. J. Mhin, U. S. Choi, and K. Lee, J. Chem. Phys. **97**, 6649 (1992).
[34] K. S. Kim, J. Y. Lee, S. J. Lee, T.-K. Ha, and D. H. Kim, J. Am. Chem. Soc. **116**, 7399 (1994); J. Y. Lee, S. J. Lee, H. S. Choi, S. J. Cho, K. S. Kim, and T.-K. Ha, Chem. Phys. Lett. **232**, 67 (1995); K. S. Kim, J. Y. Lee, H. S. Choi, J. Kim, and J. H. Jang, *ibid.* **265**, 497 (1997); P. Tarakeshwar, S. J. Lee, and K. S. Kim, J. Chem. Phys. **108**, 7217 (1998).
[35] A. K. Katz, J. P. Glusker, S. A. Beebe, and C. W. Bock, J. Am. Chem. Soc. **118**, 5752 (1996); J. Del Bene, J. Phys. Chem. **97**, 107 (1993).
[36] J. Kim and K. S. Kim, J. Chem. Phys. **109**, 5886 (1998).
[37] K. S. Pitzer, J. Chem. Phys. **7**, 251 (1939).
[38] K. S. Kim, M. Dupuis, G. C. Lie, and E. Clementi, Chem. Phys. Lett. **131**, 451 (1986); B. J. Mhin, H. S. Kim, C. W. Yoon, and K. S. Kim, *ibid.* **176**, 41 (1991); B. J. Mhin, S. J. Lee, and K. S. Kim, Phys. Rev. A **48**, 3764 (1993); J. Kim, J. Y. Lee, S. Lee, B. J. Mhin, and K. S. Kim, J. Chem. Phys. **100**, 4484 (1994); B. J. Mhin, S. J. Lee, and K. S. Kim, Chem. Phys. Lett. **219**, 243 (1994); K. A. Franken, M. Jalaie, and C. E. Dykstra, *ibid.* **198**, 59 (1992); C. J. Tsai and K. D. Jordan, *ibid.* **213**, 181 (1993); K.

Kim, K. D. Jordan, and T. S. Zwier, J. Am. Chem. Soc. **116**, 11568 (1994); J. Kim, D. Majumdar, H. M. Lee, and K. S. Kim, J. Chem. Phys. **110**, 9128 (1999), this issue.

[39] GAUSSIAN 94, Revision E. 2, M. J. Frisch, G. W. Trucks, H. B. Schlegel, P. M. W. Gill, B. G. Johnson, M. A. Robb, J. R. Cheeseman, T. Keith, G. A. Petersson, J. A. Montgomery, K. Raghavachari, M. A. Al-Laham, V. G. Zakrzewski, J. V. Oritz, J. B. Foresman, J. Cioslowski, B. B. Stefanov, N. Nanayakkara, M. Challacombe, C. Y. Peng, P. Y. Ayala, W. Chen, M. W. Wong, J. L. Andres, E. S. Replogle, R. Gomperts, R. L. Martin, D. J. Fox, J. S. Binkley, D. J. Defrees, J. Baker, J. P. Stewart, M. Head-Gordon, C. Gonzalez, and J. A. Pople, Gaussian, Inc., Pittsburgh, PA, 1995.

[40] GAUSSIAN 98, M. J. Frisch, G. W. Trucks, H. B. Schlegel, G. E. Scuseria, M. A. Robb, J. R. Cheeseman, V. G. Zakrzewski, J. A. Montgomery, R. E. Stratmann, J. C. Burant, S. Dapprich, J. M. Millam, A. D. Daniels, K. N. Kudin, M. C. Strain, O. Farkas, J. Tomasi, V. Barone, M. Cossi, R. Cammi, B. Mennucci, C. Pomelli, C. Adamo, S. Clifford, J. Ochterski, G. A. Petersson, P. Y. Ayala, Q. Cui, K. Morokuma, D. K. Malick, A. D. Rabuck, K. Raghavachari, J. B. Foresman, J. Cioslowski, J. V. Ortiz, B. B. Stefanov, G. Liu, A. Liashenko, P. Piskorz, I. Komaromi, R. Gomperts, R. L. Martin, D. J. Fox, T. Keith, M. A. Al-Laham, C. Y. Peng, A. Nanayakkara, C. Gonzalez, M. Challacombe, P. M. W. Gill, B. G. Johnson, W. Chen, M. W. Wong, J. L. Andres, M. Head-Gordon, E. S. Replogle, and J. A. Pople, Gaussian, Inc., Pittsburgh, PA, 1998.

[41] Y. Xie, R. B. Remington, and H. F. Schaefer III, J. Chem. Phys. **101**, 4878 (1994).

[42] M. E. Casida, C. Jamorski, K. C. Casida, and D. R. Salahub, J. Chem. Phys. **108**, 4439 (1998).

[43] P. Ayotte, G. H. Weddle, J. Kim, and M. A. Johnson, J. Am. Chem. Soc. **120**, 12361 (1998).

[44] O. M. Cabarcos, C. J. Weinheimer, J. M. Lisy, and S. S. Xantheas, J. Chem. Phys. **110**, 5 (1999).